RSC Advances

ROYAL SOCIETY OF CHEMISTRY

www.rsc.org/advances

Investigating the Nano-tribological Properties of Chemical Vapor Deposition-grown Single Layer Graphene on SiO_2 Substrates Annealed in Air Ambient

Quan Wang[1,2 *], Bing Bai[1], Yun Li[1],Yan Jiang[3], Laipeng Ma[4], Naifei Ren[1]

1. *School of Mechanical Engineering, Jiangsu University, Zhenjiang 212013, P.R.China*
2. *State Key Laboratory of Transducer Technology, Chinese Academy of Sciences, Shanghai 200050, P.R.China*
3. *School of Material Science & Engineering, Jiangsu University, Zhenjiang 212013, P.R.China*
4. *Shenyang National Laboratory for Materials Science, Institute of Metal Research, Chinese Academy of Sciences, Shenyang 110016, P.R. China*

Abstract

Nano-tribological properties of graphene have attracted a lot of research interest in the last few years. In this work, X-ray photoelectron spectroscopy was used to study the distribution of chemical groups in the chemical vapor deposition (CVD) single layer graphene transferred onto 90 nm SiO_2/Si substrate. It was demonstrated that the graphene was oxidized after thermal treatment at 520 ℃ in air ambient, as indicated by the formation of C=O, C-OH bond. Significantly enhanced D-band and decreased 2D-band were found in the Raman spectrum. Blue shift occurred to G-band and 2D-band after thermal oxidation. The nano-tribological properties of graphene before and after thermal oxidation were studied with atomic force microscope. A remarkable increase of friction was found on the surface of graphene after thermal oxidation. This was contributed to the increased adhesion and decreased Young's

*Author to whom correspondence should be addressed. Electronic mail: wangq@mail.ujs.edu.cn

modulus of functionalized graphene, inducing the increase of contact stiffness. In addition, the adhesion force between the tip and the samples was discussed as an important factor affecting tribological properties in nano-scale.

1 Introduction

Graphene is a two-dimensional, zero bandgap material with carbon atoms arranged in a honeycomb lattice.[1,2,3] Since graphene first became experimentally accessible in 2004,[4] it has attracted considerable research attention owing to its unique properties such as high specific surface area, ultra-high intrinsic mobility and great mechanical strength.[5,6,7]

Many recent works have concentrated on the mechanical and tribological performance of graphene.[8,9,10] Lee *et al.* found that there was a decreased friction force between SiN tip and graphene flake prepared on silicon oxide with the increasing number of graphene layers. The "puckering effect" was proposed to explain this phenomenon.[9] Filleter *et al.* found that friction force was higher on graphite compared to epitaxial bilayer graphene on SiC substrate surface, and "electron-phonon coupling" theory was presented in their work.[10] However, the large area graphene with controlled shape and layers is needed in the practical applications of graphene. Currently, the increasingly mature chemical vapor deposition (CVD) method was widely applied to the preparation of graphene which is utilized in graphene-based devices and the flexible display devices. Graphene prepared by CVD is sensitive to the impurities and ion in air ambient, such as the adsorption of H_2O,

oxygen molecules and the chemical functionalization of graphene surface in air ambient. It is not clear how doping and functionalization influence the nano-tribological properties of graphene. Therefore, it must be better understood to design the stability of graphene-based devices. Nan *et al.* studied the thermal stability of graphene in air ambient by Raman spectroscopy, and found that single layer graphene (SLG) prepared by CVD would show defects at ~500 ℃. These defects were initially SP^3 type and became vacancy-like at higher temperature.[11] However, there are few research on the change of bonding energy structure and mechanics characteristics of graphene after thermal treatment in ambient. In this paper, we present the research on the nano-tribological of graphene before and after thermal treatment in ambient.

In the term of device integration, the preparation of devices with thin gate dielectric layer has become preferred with the rapid development of CMOS process. We use the high quality SLG prepared by CVD method transferred onto Si substrate with 90 nm thermal oxidation SiO_2 in this study. X-ray photoelectron spectroscopy (XPS) was used to analyze the distribution of chemical groups in the CVD single layer graphene. It revealed that the graphene was oxidized, which was indicated by the formation of C=O, C-OH bond after annealing in ambient atmosphere at 520 ℃. This can be manifested as the appearance of a disorder-induced D-band in Raman spectrum. Then the surface topography and nano-tribological properties of graphene before and after thermal oxidation were investigated with atomic force microscopy

(AFM). These results would provide valuable information for the application of graphene-based devices.

2 Experimental

Graphene samples are prepared by CVD method. Graphene is grown on thin copper foils about 25 μm at 1000 ℃ with a flow of H_2 (30 sccm) and CH_4 (50 sccm), the growth pressure of ~100 Pa, and the growth time of 20 min. Graphene was transferred to the Si substrate with 90 nm thermal oxidation SiO_2. Optical microscopy is used to estimate the thickness, which is further confirmed by Raman spectroscopy.

As the physical or chemical adsorption of H_2O molecules on sample surface has great influence on surface properties of two-dimensional material, the samples were annealed in rapid thermal annealing furnace in N_2 atmosphere with the temperature at ~380 ℃ for 2 hours. Thermal oxidation process of graphene was carried out in STF-1200X tube furnace and the graphene samples were kept in it for 5 min at 520 ℃ in air ambient.

Raman spectra of graphene before and after thermal oxidation was recorded at room temperature by using WiTec alpha 300R system with 532 nm laser wavelength. The laser power was kept below 2 mW to avoid laser-induced heating or damage for graphene.[12] The 5 μm×5 μm Raman images was obtained by recording Raman spectrum at every point when the sample moves along the x or y axis with step size of 200 nm. X-ray photoelectron spectroscopy (XPS, K-Alpha, Thermo Scientific) was performed using amonochromated Al *K*α irradiation. The chamber pressure was about

3×10^{-8} Torr under testing conditions. Peak split and fitting of C 1s of graphene samples before and after thermal oxidation were accomplished using XPSPEAK 4.1.

The surface morphology and nano-tribological properties of different samples were measured using a MFP3D-SA atomic force microscope (AFM, Asylum Research) in contact mode. A Non-Conductive Silicon Nitride probe (Veeco NP-20, spring constant k=0.37 N/m) was employed for AFM measurements with scan rate of 1 Hz and scan angle of 90°. There are various influence factors in the measurement of nano-tribological, such as roughness of substrate,[13] scanning speed[14] *etc*. In order to improve the reliability of the experimental results, parameter settings (scan size, scan rate, scan angle *et al.*), type of probe and test environment (room environment) were kept the same in all measurements. The values of friction presented below are average value of Root-Mean-Square (RMS) obtained from scan area about 1 μm×1 μm. To obtain the adhesive force between the AFM tip and the samples surface, the force-distance curves were recorded, and the pull-off force was considered to be the adhesive force. The value of adhesion force was the average of RMS obtained from the 10 pt×10 pt force-distance map. Owing to the complexity of the calibration of the torsional force constant, and the same cantilever applied in all measurements, the output voltages were directly used as the relative frictional force.

3 Results and discussion

In order to avoid the influence of the number of graphene layers on the measurements of nano-tribological properties, Raman spectrum was used to be an

effective means for the precise representation of the number of layers of the test area. Fig. 1(b) shows the Raman spectra of pristine graphene which is the randomly selected test point in Fig 1(a), and two representative peaks of graphene observed at ~2680 cm^{-1} (2D-band) and ~1580 cm^{-1} (G-band). The intensity ratio of 2D and G peaks (I_{2D}/I_G) is >1.5, indicating that the graphene is single layer graphene (I_{2D}/I_G of bilayer and multilayer would be less than 1.5). The insert shows a single Lorentzian 2D peak with a full width at half maximum of ~30 cm^{-1} which confirms that the graphene is a SLG.[15] Fig. 1(a) presents the Raman image of the intensity ratio of 2D and G peaks for 5 μm×5 μm test area of CVD graphene. Most of the region is SLG with I_{2D}/I_G >1.5. There is no D-band observed in Fig. 1(b), indicating that there is a small amount of intrinsic defects in these pristine CVD graphene.

The Raman spectra of SLG before and after thermal treatment at 520 ℃ in air are shown in Fig. 2(b). The significant enhancement of D-band can be observed clearly due to the reaction of graphene with O_2 in the open furnace, which creates defects such as carbon-oxygen SP^3 bonds and vacancies after thermal treatment. Significant degradation and blue shift of 2D and G peaks are observed after thermal treatment in air, which is caused by the increasing defects and hole doping effect resulting from the charge transfer between adsorbed molecules (H_2O and O_2) and graphene. Fig. 2(a) shows the Raman image of intensity ratio of D and G peaks (I_D/I_G) is 0.2~0.4, indicating the induced defects are uniformly distributed after thermal treatment.[16,17]

In order to determine the defect types of graphene and distribution of bond energy before and after thermal treatment in air, XPS analysis was carried out to substantiate directly whether the graphene was oxidized or not after thermal treatment in air ambient. Fig. 3(a) shows the C 1s of pristine graphene. A typical signal at C-C (284.5 eV) was obtained through Gaussian fitting. Fig. 3(b) shows XPS spectrum of C 1s for graphene after thermal treatment in air can be deconvoluted into three Gaussian peaks, which are typical signals of C-C (284.5 eV), C-OH (285.6 eV), and C=O (288.4 eV). XPS analysis fully demonstrates that graphene was oxidized faintly with generating of SP^3 hybridization after thermal treatment at 520 ℃ in air ambient.

Fig. 4(a) presents the morphology of pristine graphene on 90 nm SiO_2/Si. The ripples, originating from the cool-down and transfer process of the sample preparation, are shown in the morphology. Moreover, a small quantity of residuals of the PMMA resist appear as highly protruding objects. Figs. 4(b) and 4(c) present the trace and retrace image of friction. To identify graphene on substrate, friction image is more effective compared with morphology image. Shown in Fig. 4(d), the friction loop is consisted of trace and retrace friction force profiles of the line. The width of the loop can be used to roughly represent the practical friction of different area, indicating that friction on SiO_2 is about four times larger than that on graphene.

Compared with Fig. 4(a), Fig. 5(a) gives a more micromesh morphology image of the wrinkles of pristine graphene clung gently on the substrate. The wrinkles would be preserved if they existed before the graphene was transferred to the target substrate. [18] In addition, SLG, clung on the substrate by the weak van der Waals force interaction

with substrate, could also exist folded structure.[19] Moreover, residuals between graphene and substrate in transferred process is a main factor for the influence of topography of graphene on substrate. The presence of the winkles and bubbles also caused the change of friction between tip and sample with fluctuation of the surface of sample, indicating nano-tribological test is associated with the roughness of the surface, as is shown in Figs. 5(b) and 5(c). The surface become smoother after thermal treatment in air, supported as the values of mean square roughness values (*R*a) from 0.85 nm to 0.44 nm. The flexible PMMA on graphene become stiffness after thermal treatment, resulting in a larger friction, shown as the light and black spot in Figs. 5(e) and 5(f), respectively. In order to minimize the influence of changing morphology on the test of nano-tribological, all of the friction data presented below are average values of Root-Mean-Square (RMS) obtained from scan area about 1 μm×1 μm.

Fig. 6 shows the changes of friction between tip and graphene versus varied load. The relative friction coefficients (RFC) of friction for graphene before and after oxidized can be extracted from the slopes of the fitting lines in Fig. 6. There is an obvious enhancement of RFC of the graphene after oxidized, observed in the Fig. 6. It is noted that the friction of both samples could not be zero despite without normal load. According to the Amonton's law, the friction between tip and sample can be expressed as follow in nanoscale:[20]

$$L_f=\mu(L_{load}+L_{adh}), \quad (1)$$

where μ is friction coefficient. L_{load} and L_{adh} are the normal load and the adhesion force between the two objects. Due to the biggish load $L_{load} \gg L_{adh}$, the effect of adhesion force on friction can be neglected in the measurements of macroscopical friction. But L_{load} (about 0~30 nN in this research) is equal to L_{adh} (about 0~100 nN with our measurements) in the measurements in nano-tribological. So L_{adh} is crucial for the characterization of nano-tribological, especially the two-dimensional material with excellent elastic properties. In this work, when $L_{load}=0$, L_{adh} plays the role of L_{load}, leading to the so-called "initial friction".

Fig. 7 shows the statistics histogram of friction signals and adhesion force for pristine graphene, oxygenated graphene and 90 nm SiO_2/Si substrate. There is a significant increase of friction and adhesion on graphene after oxidation. But it is much smaller compared to the substrate, indicating that graphene can be an excellent solid lubricant whether it is oxidized or not. The corresponding relationship between the change of friction and adhesion suggests that adhesion is a decisive factor in the nano-tribological.

There are several possible mechanisms proposed for the nano-tribological behavior of graphene, such as the energy dissipation mechanism,[21] the mechanism of electron phonon coupling[9] and "puckering effect".[8,22] Due to the inseparable relationship between friction in nano-scale and the elastic property of material,[23] the exchange of mechanical property with graphene after chemical modification cannot be neglected on the impact of its tribological property.

The nanoscale friction force in the lateral force microscope (LFM) stick-slip motion is determined by the slope of the LFM profile (the total lateral stiffness) on the measurements of nano-tribological property of graphene clung on the substrate with AFM.[24] The relationship between total lateral stiffness is and the friction signal (Torsion of the probe) can be expressed as[25]

$$\frac{dF_{\text{lateral}}}{d_x} = k_{\text{total}} = \left[\frac{1}{k_{\text{lever}}} + \frac{1}{k_{\text{graphene-substrate}}} + \frac{1}{k_{\text{tip-graphene}}}\right]^{-1}. \quad (2)$$

$k_{\text{graphene-substrate}}$ is large enough to be neglected in Eq. (2) when graphene and substrate interact with each other tightly, and k_{lever} is not be considered because the same lever was used in this experiment. The contact stiffness determined by the lateral deformation in the tip-to-graphene contact as the sole variable in Eq. (2) can be expressed as

$$k_{\text{tip-graphene}} = 8G^{*}a, \quad (3)$$

where G^{*} can be calculated by $G^{*} = \left[\left(2\text{-}\nu_1\right)^2/G_1 + \left(2\text{-}\nu_2\right)^2/G_2\right]^{-1}$. G_1 and G_2, ν_1 and ν_2 are shear modulus and Poisson ratio of silicon nitride tip and graphene, respectively. a is the contact radius between tip and sample which can be expressed with Hertz theory:

$$a = \left[\frac{3R}{4E^{*}}(L_{\text{load}} + L_{\text{adh}})\right]^{1/3}, \quad (4)$$

where $E^{*} = \left[\left(1\text{-}\nu_1\right)^2/E_1 + \left(1\text{-}\nu_2\right)^2/E_2\right]^{-1}$. E_1 and E_2 are the Young's modulus (elasticity modulus) of silicon nitride tip and graphene respectively. R is the radii of curvature (ROC) for AFM probe tip, L_{load} is the normal load applied by the tip and L_{adh} is the adhesion force between tip and sample. Young's modulus of pristine SLG

prepared by mechanical exfoliation is ~1.0 TPa [6] and SLG prepared by chemical reduction of graphene oxide is ~0.25±0.15 TPa.[26] Paci *et al.* have proved that the oxidation of graphene will lead to a greatly reduce of its Young's modulus and breaking strength.[27] Due to the decreasing of Young's modulus of graphene and the increasing of adhesion force between tip and sample, with the consideration of Eq. (2) ~ (4), there would be a larger total lateral stiffness k_{total} when the tip slip on the graphene after oxidized. Therefore, an increasing friction signal can be observed by AFM.

As discussed above, the adhesion between tip and sample is a significant factor in nano-tribological tests with AFM. In other words, it also can be considered as an additional load. It is well-known that environment change for a short period of time is not easy to cause the functionalization of surface. But there would be a strong impact on the chemical bond on the surface of graphene because of the interaction with the gas and ion in the air. Therefore, it is imperative to know the influence of environment in the adhesion force on the graphene surface. Q. Li *et al* found that the adhesion force between tip and mechanical exfoliated multilayer graphene was increased with the increase of the time exposed to the air, resulting a larger friction on the surface of graphene.[28]

The adhesion force is generally consists of capillary force L_C, van der Waals force L_{vdW}, electrostatic force L_E and bonding force L_B which can be expressed as

$$L_{adh}=L_C+L_{vdW}+L_E+L_B. \quad (5)$$

Because the samples and the probes have placed in air for a long time, there is no

additional charge on the surface. The surfaces of the tip and samples are saturated with chemical bonds, L_E and L_B can be neglected in this research. Herein, L_C and L_{vdW} are the main factors in the influence of adhesion between tip and graphene before and after thermal oxidation.

L_C is a main contributor to adhesion and closely related to surface wettability. SP^3 hybridization was introduced in pristine graphene after thermal oxidation and C-OH bonds were formatted on the surface of graphene. Due to the function of hydrogen bond, water vapor in the air is easy to be adsorbed on the surface, leading to the enhancement of capillarity between tip and sample. In addition, the contact area between graphene and substrate was increased after thermal oxidation (winkles and bubbles were decreased). The van der Waals force is increased because the interaction between tip and substrate is enhanced, as the Lennard-Jones potential strengthen with λ^{-6}, where λ is the distance between tip and substrate. The van der Waals interaction between tip and SiO_2 is much stronger than that of graphene. And hence, large L_C and L_{vdW} may be the key factor in the relatively high adhesion as is shown in Fig. 7.

4 Conclusions

In this work, high-quality single layer graphene prepared by CVD were transferred onto 90 nm SiO_2/Si substrate. Thermal treatment for the transferred graphene was taken at 520 ℃ in air ambient. The microstructure and tribological properties of the samples were investigated. These results show that the graphene

were oxidized, as indicated by the formation of C=O, C-OH bond after annealed in air atmosphere. A significant increase of friction was found on the surface of graphene which is attributed to the decreased Young's modulus and increased adhesion after thermal oxidation. The adhesion force between tip and samples was discussed as an important factor on affecting of tribological properties in nano-scale.

ACKNOWLEDGMENTS

This work was supported by the National Natural Science Foundation of China (No. 51175238), the Industrial Supporting Plan of Zhenjiang City (No.GY2013011), "Six talent peaks" of high level talent selection and training project of Jiangsu Province（No. 2013-ZBZZ-031）, the Priority Academic Program Development of Jiangsu Higher Education Institutions and Graduate research and innovation projects in Jiangsu University (No.KYXX_0029). The authors would like to thank Rong Ding, from Taizhou Sunano New Energy Co., Ltd for his technical direction and support in Raman spectrometry. Laipeng Ma, from Institute of Metal Research (IMR), CAS, is appreciated for the graphene sample transfer to our substrates and he acknowledges the support from NSFC (No.51102241) and MOST (No.2012AA030303).

Reference

1. K. S. Novoselov, A. K. Geim, S. V. Morozov, D. Jiang, M. I. Katsnelson, I. V. Grigorieva, S. V. Dubonos, and A. A. Firsov, Nature **438**, 197 (2005).
2. A. K. Geim, Science **324**, 1530 (2009).
3. Y. Zhang, Y. W. Tan, H. L. Stormer, and P. Kim. Nature **438**, 201 (2005).
4. K. S. Novoselov1, A. K. Geim, S. V. Morozov, D. Jiang, Y. Zhang, S. V. Dubonos, I. V.

Grigorieva, and A. A. Firsov, Science **306**, 666 (2004).

5. J. H. Chen, C. Jang, S. Xiao, M. Ishigami, and M. S. Fuhrer, Nature Nanotechnology **3**, 206 (2008).
6. C. Lee, X. Wei, J. W. Kysar, and J. Hone, Science **321**, 385 (2008).
7. G. Xie, M. Forslund, and J. Pan. ACS Applied Materials & Interfaces **6**, 7444 (2014).
8. Y. Jiang, Y. Li, B. Liang, X. Yang, T. Han, Z. Wang, Nanotechnology **23**, 495703 (2012).
9. C. Lee, Q. Li, W. Kalb W, X. Z. Liu, H. Berger, R. W. Carpick, and J. Hone, Science **328**, 76 (2010).
10. T. Filleter, J. L. McChesney, A. Bostwick, E. Rotenberg, K. V. Emtsev, Th. Seyller, K. Horn, and R. Bennewitz, Phys. Rev. Lett. **102**, 086102 (2009).
11. H. Nan, Z. Ni, J. Wang, Z. Zafar, Z. Shi, and Y. Wang, Journal of Raman Spectroscopy **44**, 1018 (2013).
12. D. Teweldebrhan, V. Goyal, and A. A. Balandin, Nano Letters **10**, 1209 (2010).
13. E. SuáKim, and S. YoonáLee, Nanoscale **5**, 3063 (2013).
14. J. Chen, I. Ratera, J. Y. Park, and M. Salmeron, Phys. Rev. Lett **96**, 236102 (2006).
15. A. C. Ferrari, J. C. Meyer, V. Scardaci, C. Casiraghi, M. Lazzeri, F. Mauri, S. Piscanec, D. Jiang, K. S. Novoselov, S. Roth, and A.K. Geim, Phys. Rev. Lett. **97**, 187401 (2006).
16. H. Xu H, Y. Chen, J. Zhang, and H. Zhang, Small **8**, 2833 (2012).
17. Z. H. Ni, H. M. Wang, Z. Q. Luo, Y. Y. Wang, T. Yu, Y. H. Wu, and Z. X. Shen, Journal of Raman Spectroscopy **41**, 479 (2010).
18. G. H. Han, F. Güneş, J. J. Bae, E. S. Kim, S. J. Chae, H. J. Shin, J. Y. Choi, D. Pribat, and Y. H. Lee, Nano Letters **11**, 4144 (2011).

19. M. Ishigami, J. H. Chen, W. G. Cullen, M. S. Fuhrer, and E. D. Williams, Nano Letters **7**, 1643 (2007).

20. G. Xie, J. Ding, B. Zheng, W. Xue. Tribology International, **42**, 115-121(2009).

21. A. Smolyanitsky, J. P. Killgore, and V. K. Tewary, Phys. Rev. B **85**, 035412 (2012).

22. J. S. Choi, J. S. Kim, I. S. Byun, D. H. Lee, M. J. Lee, B. H. Park, C. Lee, D. Yoon, H. Cheong, K. H. Lee, Y. W. Son, J. Y. Park, and M. Salmeron, Science **333**, 607 (2011).

23. S. Kwon, J. H. Ko, K. J. Jeon, Y. H. Kim, and J. Y. Park, Nano Letters **12**, 6043 (2012).

24. R. W. Carpick, D. F. Ogletree, and M. Salmeron, App. Phys. Lett **70**, 1548 (1997).

25. J. Colchero, M. Luna, and A. M. Baro, Appl. Phys. Lett 68, 2896 (1996).

26. C. Gómez-Navarro, M. Burghard, and K. Kern, Nano Letters **8**, 2045 (2008).

27. J. T. Paci, T. Belytschko, and G. C. Schatz, The Journal of Physical Chemistry C **111**, 18099 (2007).

28. Z. Deng, A. Smolyanitsky, Q. Li, X. Q. Feng, and R. J. Cannara, Nature materials **11**, 1032 (2012).

Captions of figures

Fig.1. Raman spectrum of pristine SLG with small amount of intrinsic defects. (a) is the Raman image of the intensity ratio of 2D and G peaks(I_{2D}/I_G). (b) is the Raman spectrum fitted by Lorentz. The insert gives the Lorentz fitting of 2D peak.

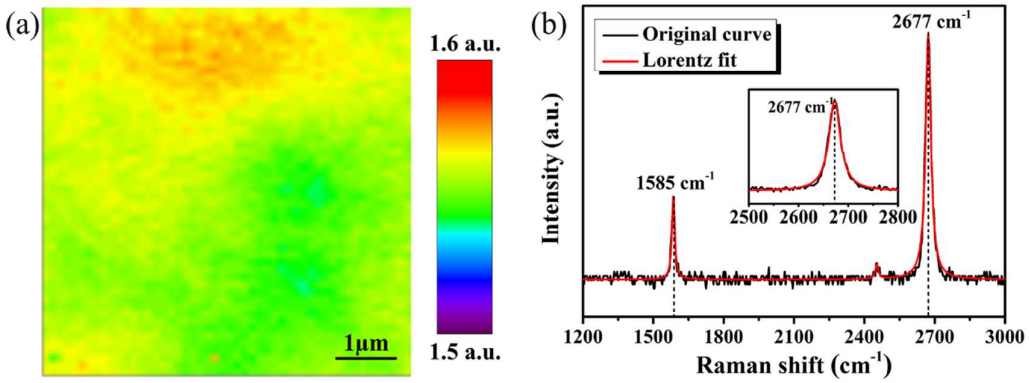

Fig.2. (a) is the Raman image of the intensity ratio of D and G band (I_D/I_G) of thermal treated graphene. (b) is the Raman spectra of SLG by CVD before and after thermal treatment at 520 ℃ in air ambient.

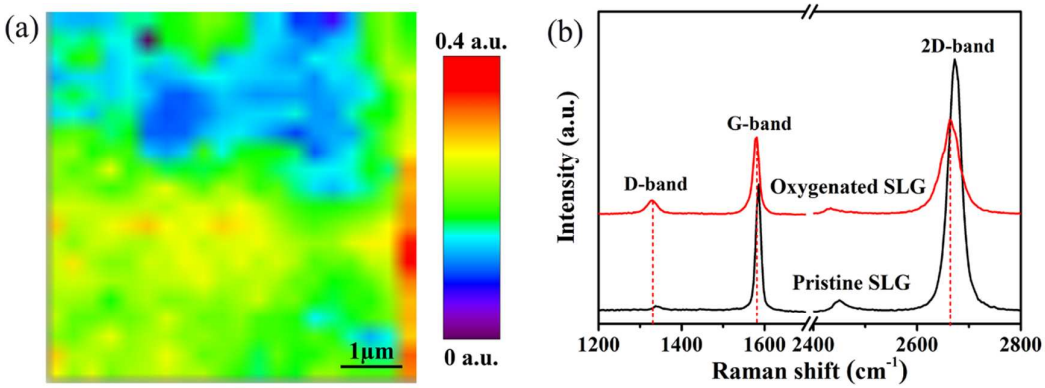

Fig.3. XPS spectra of C 1s for graphene (a) before and (b) after thermal treatment at 520 ℃ in ambient atmosphere, the ratio between C=C, C-OH, and C=O is 10:3:1.

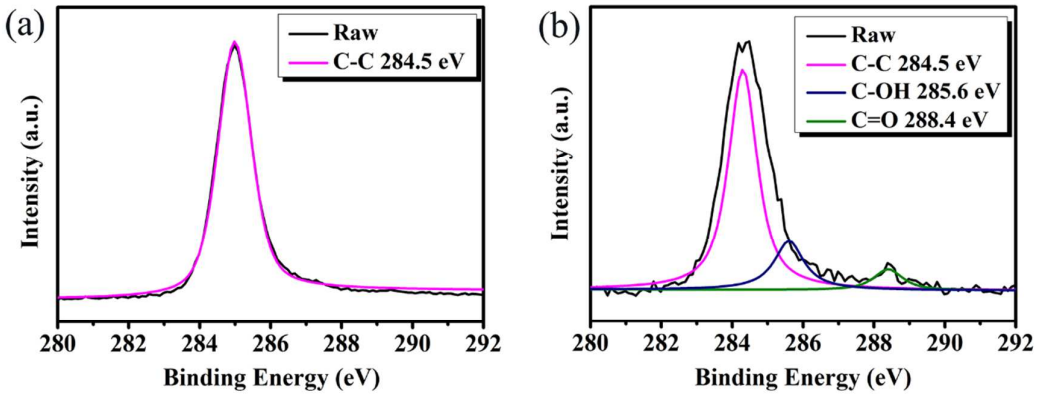

Fig.4. (a) is the morphology image of pristine graphene on 90 nm SiO_2/Si. (b) and (c) are the trace and retrace image of friction. (d) is friction value line profiles obtained from forward and backward scans across SiO_2 and SLG. The position of scan line is shown in (a) (green line), (b) (black line) and (c) (red line), respectively. The scan size is 10 μm×10 μm and the color bar used in (b) and (c) is the same one.

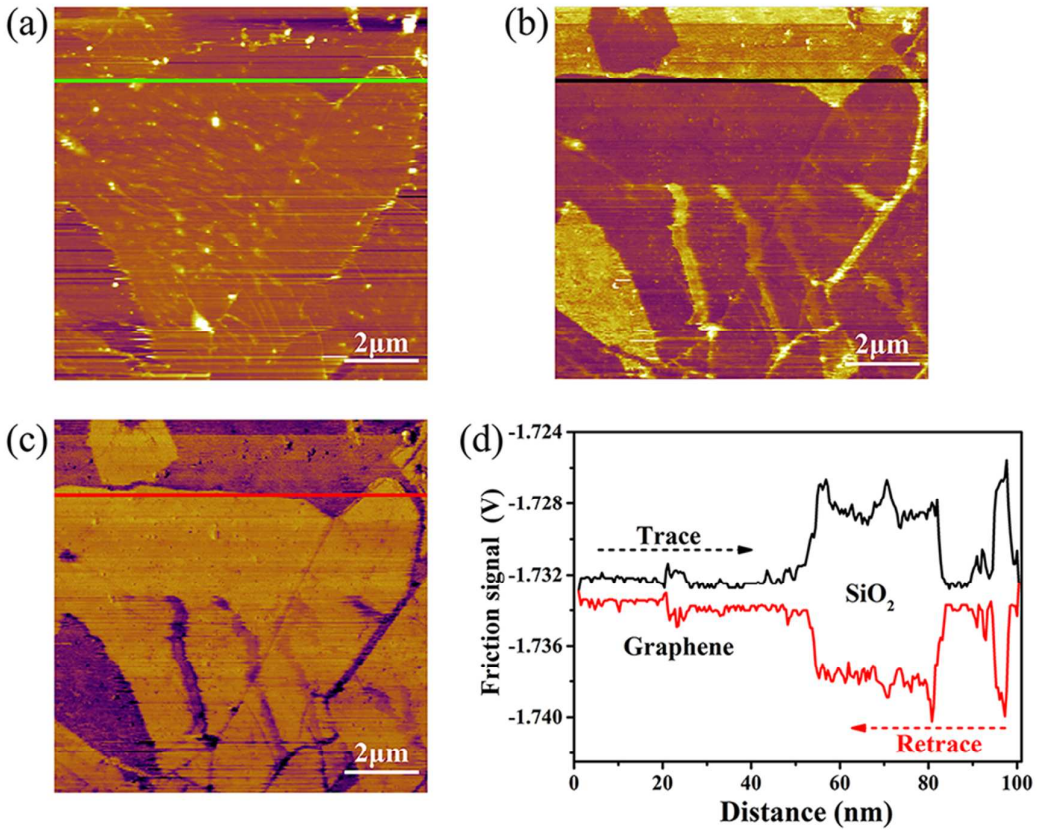

Fig. 5. (a) and (d) are the morphology images of graphene on SiO_2/Si substrate before and after thermal oxidation respectively. Followings are the friction images of (b) (e) trace and (c) (f) retrace direction corresponding to (a) and (b), respectively.

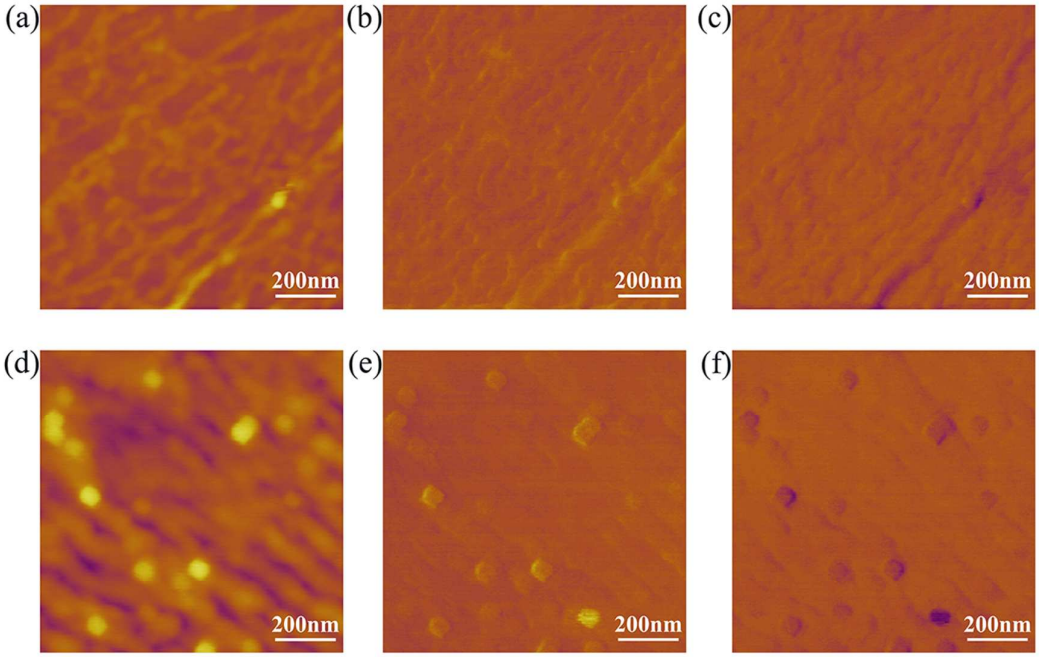

Fig 6. A graph showing the effect of varying load on the friction force (measured as the width of the lateral deflection loop). Error bars represent the standard deviation of collected data.

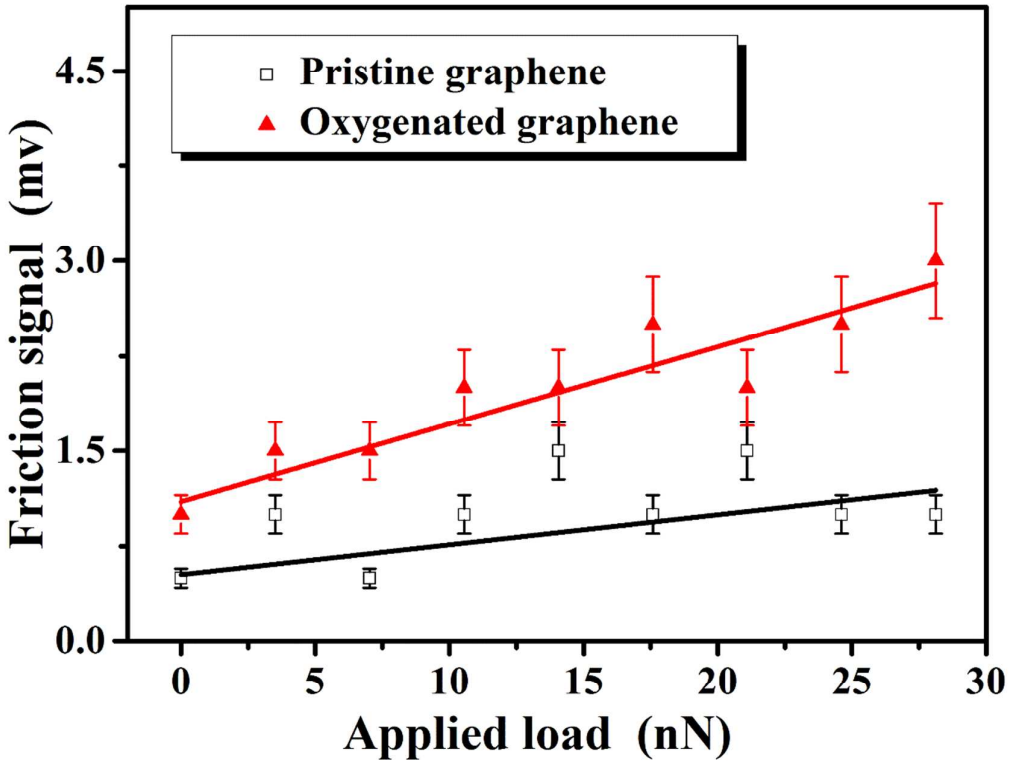

Fig.7. Comparison of friction signals and adhesion force for pristine graphene, oxygenated graphene and 90nm SiO_2/Si substrate (normal load = 7 nN). Error bars represent the standard deviation of collected data.